Chemical Engineering Journal 163 (2010) 62–67

Contents lists available at ScienceDirect

Chemical Engineering Journal

journal homepage: www.elsevier.com/locate/cej

# $TiO_2$/HZSM-5 nano-composite photocatalyst: HCl treatment of NaZSM-5 promotes photocatalytic degradation of methyl orange

Wenjie Zhang [a,*], Kuanling Wang [a], Yang Yu [a], Hongbo He [b]

[a] School of Environmental and Chemical Engineering, Shenyang Ligong University, Shenyang Hun-Nan, Shenyang 110159, China
[b] Institute of Applied Ecology, The Chinese Academy of Sciences, Shenyang 110016, China

ARTICLE INFO

*Article history:*
Received 7 May 2010
Received in revised form 15 July 2010
Accepted 19 July 2010

*Keywords:*
Photocatalysis
$TiO_2$
HZSM-5
Methyl orange

ABSTRACT

$TiO_2$/HZSM-5 nano-composite photocatalysts were prepared by dispersing $TiO_2$ onto the surface of HCl-treated NaZSM-5 zeolite using a sol–gel method. These materials were characterized by scanning electron microscopy (SEM), X-ray diffraction (XRD), Fourier transform infrared spectroscopy (FT-IR), BET surface area analysis and X-ray photoelectron spectroscopy (XPS) measurements. Photocatalytic activities of the supported catalysts were examined through methyl orange degradation under UV irradiation. The results showed that HCl modification of NaZSM-5 did not noticeably change the surface morphology and structure of the zeolite. Improved dispersion and restrained crystalline size of $TiO_2$ could be found after supporting the $TiO_2$ on HZSM-5. Ti–O–Si bonds did not form between the HZSM-5 bulk and the supported $TiO_2$. Supported $TiO_2$ calcinated at 400 °C presented anatase structure. The titanium was in the oxidation state of $Ti^{4+}$, and the oxygen was in the form of $O^{2-}$ in both $TiO_2$ and $SiO_2$. The adsorption ability and photocatalytic degradation activity of $TiO_2$/HZSM-5 nano-composite were better than that of bare $TiO_2$, accompanied with increasing specific surface area. Meanwhile, photocatalytic degradation activity of $TiO_2$/HZSM-5 changed remarkably when HZSM-5 supports treated with different concentrations of HCl were used, giving the optimum HCl concentration of 0.3 mol/l. The recycling of $TiO_2$/HZSM-5 photocatalyst was also investigated and methyl orange degradation rate was 82.4% of the initial rate after three recycles.



## 1. Introduction

Heterogeneous photocatalysis based on $TiO_2$ has attracted much attention because of its application in the eliminations of aqueous pollutants [1–3]. $TiO_2$ has showed many good aspects such as high activity, low cost and chemically stable and has been applied to a variety of environmental problems as a main photocatalyst especially in water and air purification [4–6]. Under exposure of light irradiation, $TiO_2$ can produce highly oxidative hydroxyl radical that can in turn result in thorough oxidation of most organic pollutants into final products of $CO_2$, $H_2O$ and other inorganic ions [7]. An obstacle in the application of $TiO_2$ powder is that small photocatalyst particles make the separation process difficult after water treatment when the photocatalyst is used as slurry.

$TiO_2$ nanostructure plays crucial role in photocatalytic degradation activity [8–10]. The dispersion of $TiO_2$ on solid supports is to make $TiO_2$ in fine particles and to utilize the supports' adsorption ability. Certainly, dispersion of $TiO_2$ on solid supports also facilitates the recovery of photocatalyst from huge volume of treated water. Several kinds of deposition methods can be used to immobilize $TiO_2$ onto different kinds of supports. Interactions between $TiO_2$ and support may lead to enhanced photocatalytic activity [11–13]. The support can also help on concentrating pollutants to the photocatalyst surface [14–16].

Zeolites are considered to be important supports owing to their high surface area, high thermal stability and eco-friendly nature. Zeolites are also reported to provide specific photophysical properties such as control of charge transfer and electron transfer processes [17–19]. A review of recent research revealed that several zeolites such as HZSM-5 [20], Y-zeolite [21], H-mordenite [22], mesoporous Al-MCM-41 [23], and clinoptilolite [24] are successful supports for titanium dioxide. The composite photocatalysts were proved effective for degradation and mineralization of herbicides or pesticides.

ZSM-5 zeolite, with highly ordered micropores, surface acidity, and ion-exchange capacities, is one of the most widely applied inorganic materials as catalyst support, adsorbent, and molecular-sized space for various chemical or photochemical reactions [25–27]. In this article, we concern the photocatalytic decomposition of methyl orange (MO) over nano-composite photocatalysts that are prepared by dispersing $TiO_2$ on a series of HCl-modified NaZSM-5 zeolites. Considering the relatively small pore size of ZSM-5 zeolite

* Corresponding author. Tel.: +86 24 83978969.
*E-mail address:* metalzhang@yahoo.com.cn (W. Zhang).

1385-8947/$ – see front matter © 2010 Elsevier B.V. All rights reserved.
doi:10.1016/j.cej.2010.07.042

(0.4–0.7 nm), most of the photocatalytic degradation reaction must take place on the surface of the compound photocatalyst. Thus, it is worthwhile to investigate the effect of the surfaces and interaction between $TiO_2$ and ZSM-5 zeolite as well. With this purpose, results about the structure, crystal size, phase composition, morphology, BET surface area and photocatalytic activity of the prepared photocatalysts are reported.

## 2. Experimental

### 2.1. HCl treatment of NaZSM-5

Zeolite NaZSM-5 ($SiO_2/Al_2O_3 = 50$) was obtained from Nankai Catalyst Corporation, China. Chemical composition of the zeolite is 2.1–2.3% $Na_2O$, 2.3–2.5% $Al_2O_3$, and 86.0–87.0% $SiO_2$.

HZSM-5 was prepared by HCl treating of NaZSM-5. 50 g of NaZSM-5 zeolite was put into a 1-l flask containing 500 ml different concentrations of HCl aqueous solution. The reaction was maintained at 92–95 °C for 4 h under stirring. The solid–liquid mixture was filtrated afterwards, and the zeolite was cleaned with diluted water. A $AgNO_3$ test was applied to make sure that no $Cl^-$ ion remained in the zeolite. The zeolite HZSM-5 was dried at 110 °C for 12 h. After grinding, the HZSM-5 was calcinated at 550 °C for 4 h for activation. These supports were denoted as $\chi$HZSM-5, where $\chi$ is the HCl concentration.

### 2.2. Photocatalyst preparation

$TiO_2/\chi$HZSM-5 catalysts were prepared according to a sol–gel process by the following method. Tetrabutyl titanate($Ti(OBu)_4$) was added to the $\chi$HZSM-5 suspended ethanol solution under continuous magnetic stirring. Another solution containing deionized water and ethanol was slowly added to the above-mentioned mixed slurry to hydrolyze tetrabutyl titanate adsorbed on $\chi$HZSM-5 particles, and then the resulting slurry was still under continuous magnetic stirring until it became a gel. The gel was dried at 90 °C for 12 h and calcinated at 400 °C for 2 h. Finally, the catalysts were grinded into fine powder and stored in the dark. The maximum methyl orange decolorization activity was achieved with 30 wt% loading of $TiO_2$. The catalyst, hereafter named as $30\%TiO_2/\chi$HZSM-5, was employed as a template in this study.

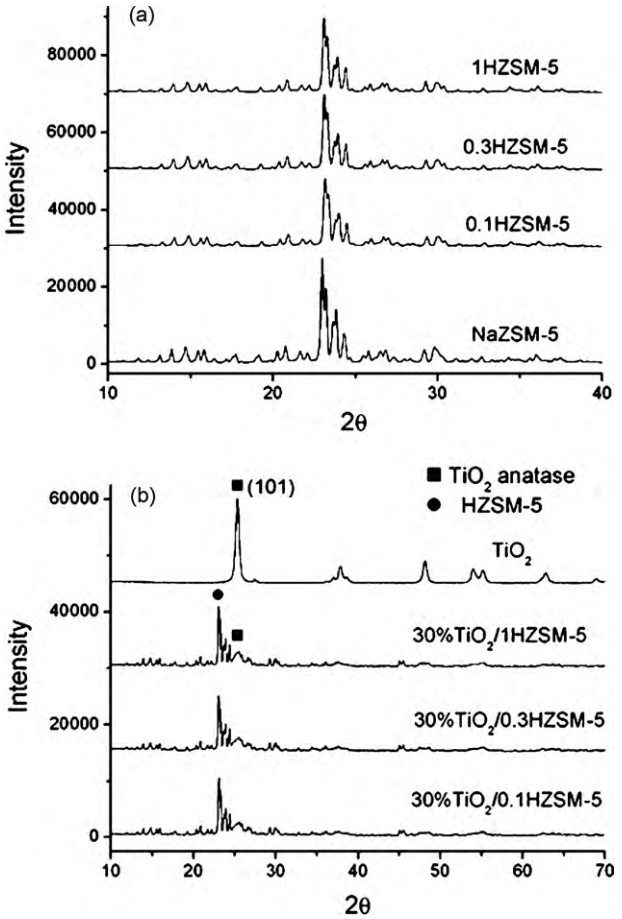


**Fig. 1.** XRD patterns of (a) ZSM-5 and (b) $30\%TiO_2/\chi$HZSM-5.

### 2.3. Characterization of photocatalyst

The crystalline structure of the photocatalyst was measured using X-ray diffraction (XRD, D/max-rB) with a Cu K$\alpha$ source. The samples were analyzed in a $2\theta$ range of 10–80° to identify the crystalline phase and also to assess the structural integrity of zeolite samples during the course of photocatalyst preparation. The surface morphology was observed by scanning electron microscope (SEM, Hitachi S-3400N). The samples for SEM imaging were coated with a thin layer of gold film to avoid charging. IR spectra of the samples were recorded using FT-IR spectrometer (WQF-410) with KBr pellets. The samples were analyzed in the wavenumber range of 4000–400 $cm^{-1}$. The titanium oxidation state was determined using X-ray photoelectron spectroscopy (XPS, MULTILAB2000). The BET specific surface area was measured by $N_2$ adsorption at low temperature on surface area analyzer (F-Sorb 3400).

### 2.4. Photocatalytic reaction

Prior to photocatalytic experiment, methyl orange adsorption in the dark on the $TiO_2$/HZSM-5 photocatalyst was measured in the suspension. 50 ml of 10 mg/l methyl orange aqueous solution was mixed with the photocatalyst in a 250 ml beaker. The suspension was stirred magnetically for 25 min to reach adsorption equilibrium. After that, 5 ml suspension was taken out of the reactor and filtrated through a Millipore filter (pore size 0.45 μm) to remove the photocatalyst. Finally, absorbency of the solution was measured by a 721E spectrophotometer at the maximum absorption wavelength of methyl orange (468 nm). The removal rate of methyl orange was calculated by the following equation [16]:

$$\eta = \frac{C_0 - C}{C_0} = \frac{A_0 - A}{A_0} \times 100\%$$

where $C_0$ and $A_0$ are the initial concentration and absorbency of methyl orange solution; $C$ and $A$ are the concentration and absorbency of methyl orange solution after a certain time.

Photocatalytic activities of the prepared catalysts were evaluated in a photocatalytic reactor. A 20 W UV lamp was located at the top of a 250 ml beaker with the distance of 15 cm. The lamp can irradiate UV light at wavelength of 253.7 nm with the intensity of 1100 μW/$cm^2$. In each experiment, 50 ml of 10 mg/l methyl orange aqueous solution was put into a 250 ml beaker. The concentration of $TiO_2$ was indicated below. In prior to turn on the lamp, the solution was magnetically stirred for 25 min to ensure adsorption equilibrium. The suspensions were filtrated through the Millipore filter before measuring. If not indicated, the irradiation time in the subsequent experiments was set to 30 min.

## 3. Results and discussion

### 3.1. Characterization of photocatalysts

XRD patterns of $\chi$HZSM-5 zeolites and $30\%TiO_2/\chi$HZSM-5 ($\chi = 0.1, 0.3, 1$) nano-composites are presented in Fig. 1. HCl treat-

**Table 1**
Si/Al ratios of NaZSM-5 and χHZSM-5.

| Sample | NaZSM-5 | 0.1HZSM-5 | 0.3HZSM-5 | 1HZSM-5 | 2HZSM-5 |
|---|---|---|---|---|---|
| $n$(Si)/$n$(Al) | 35 | 41 | 45 | 49 | 57 |

ment and dispersion of $TiO_2$ on χHZSM-5 did not damage the zeolite's structure that is characterized by three main peaks at 2θ equal to 23.18°, 23.99°, and 24.45°. The crystallinity of the resulting HZSM-5 decreased since dealumination of ZSM-5 occurred on HCl treatment.

Compared with XRD pattern of pure χHZSM-5 zeolite, intensities of diffraction peaks of 30%$TiO_2$/χHZSM-5 decreased or disappeared, since the surface of zeolite was covered by $TiO_2$. The characteristic XRD peak of anatase was observed at $2\theta = 25.3°$ for $TiO_2$ supported on χHZSM-5, and no significant rutile peak was observed, showing that rutile phase did not form on the surface of zeolite.

Surface morphologies of χHZSM-5 and 30%$TiO_2$/χHZSM-5 (χ = 0.1, 0.3, 1) are shown in Fig. S1. It is obvious that the surface of χHZSM-5 is relatively smooth (Fig S1a–c). After treating with different concentration of HCl, there was no visible change in particle size as evidenced from SEM. χHZSM-5 zeolite particle size is in the range of 0.5–5 μm. As a supporter, it can be easily separated from the treated wastewater. At the same time, the particle size is still small enough for good dispersion in the wastewater. The SEM images of 30%$TiO_2$/χHZSM-5 composites (Fig S1d–f) became rough after loading $TiO_2$ on χHZSM-5 zeolites.

The analysis of Si and Al elements was performed by energy dispersive spectroscopy in microarea, as shown in Table 1. The Si/Al ratios increased with increasing HCl concentration during treatment. It is proved that dealumination of ZSM-5 occurred after HCl treatment. This helps in increasing the surface area and loading of methyl orange.

The XPS spectra of the Ti2$p$ region for the surface of pure $TiO_2$ and 30%$TiO_2$/0.3HZSM-5 are shown in Fig. 2. Only Ti(IV) is found in pure $TiO_2$ and 30%$TiO_2$/0.3HZSM-5. A main doublet composed of two symmetric peaks situates at Eb(Ti2$p_{3/2}$) = 457.6 eV and Eb(Ti2$p_{1/2}$) = 463.4 eV is assigned to Ti(IV) [28] in both of the spectra of pure $TiO_2$ and 30%$TiO_2$/0.3HZSM-5. The O1s spectrum of $TiO_2$ has only one peak at Eb(O1s) = 529.4 eV. The O1s spectrum of 30%$TiO_2$/0.3HZSM-5 has two bands, centered at 532.4 and 528.9 eV. The former band corresponds to oxygen from $SiO_2$ of the zeolite [29] and the latter is assigned to the combination of oxygen species from $TiO_2$ [30]. It is suggested that titanium is in the oxidation state of $Ti^{4+}$, and oxygen is in the form of $O^{2-}$ in both $TiO_2$ and $SiO_2$.

Fig. 3 shows FT-IR spectra of the supported $TiO_2$ and the zeolite treated at different concentration of HCl. The region at 3150–3700 $cm^{-1}$ is attributed to the hydroxyl stretching region of zeolitic water, whose intensity decreases after HCl treatment due to dehydrate of the zeolite. The strongest absorption peak at 1047 $cm^{-1}$, which is unchanged after 1 mol/l HCl treatment, is assigned to the framework stretching vibration band of Si(Al)–O in tetrahedral Si(Al)$O_4$ in the zeolite, indicating that zeolite structure is not destroyed. The structural bands at 450–900 $cm^{-1}$ are responsible for the stretching vibrations of T–O, T–O–T, and O–T–O bonds in tetrahedral $SiO_4$ and $AlO_4$. At the same time, no obvious band can be observed at the region of 950–960 $cm^{-1}$ that is assigned to the antisymmetric stretching vibration of Ti–O–Si bond [31]. It is suggested that no strong chemical interaction takes place between $TiO_2$ and the zeolite, hence $TiO_2$ maybe disperse on the surface of the zeolite, or encapsulate partly the zeolite cavity.

To measure the crystalline sizes of $TiO_2$ nanoparticles, the $d$ (1 0 1) spacing at 25.52 (2θ) for anatase is used. X-ray peak broadening is analyzed by employing Scherrer's equation. The average crystalline sizes of supported $TiO_2$ nanoparticles are around 19 nm,

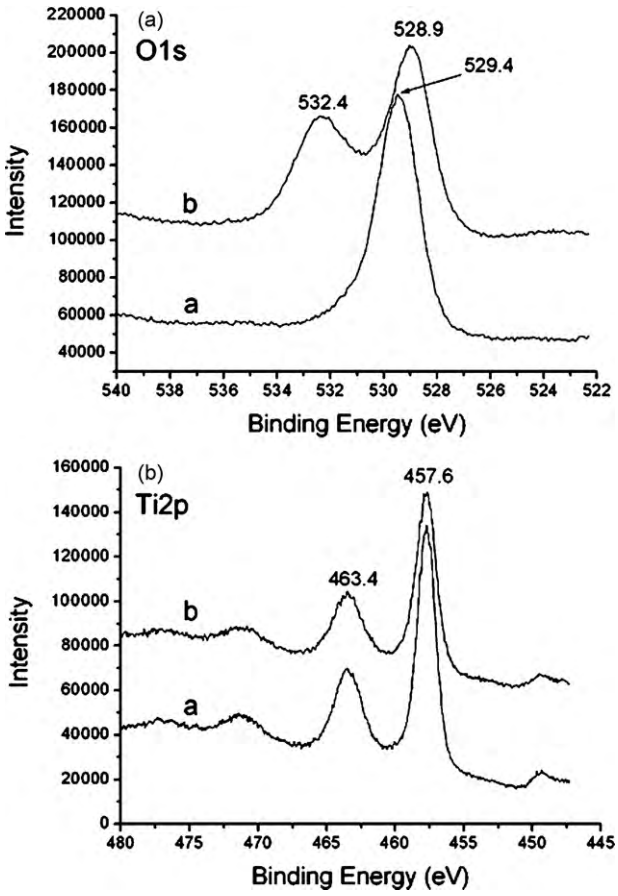


**Fig. 2.** XPS spectra of Ti2$p$ and O1s of (a) $TiO_2$ and (b) 30%$TiO_2$/0.3HZSM-5.

which is smaller than 45.2 nm of bare $TiO_2$, as indicated in Table 2. Improved dispersion and restrained crystalline size of $TiO_2$ can be found after supporting the photocatalyst on χHZSM-5. The BET surface areas of the pure NaZSM-5, χHZSM-5 and $TiO_2$ loaded on the zeolites are shown in Table 2. The surface area of the zeolite increased with increasing HCl concentration during treatment. After loading $TiO_2$ on the χHZSM-5, the surface area of all the supported catalysts decreased as compared to pure χHZSM-5. Titanium dioxide particles were deposited on the surface of the zeolites and subsequently partially blocked the pores [32], resulting in the decrease of the surface area. However, the supported catalysts still possess much higher surface area than the bare $TiO_2$.

When contacted with methyl orange in the dark, 30%$TiO_2$/χHZSM-5 nano-composites showed different adsorption capacities. The bare $TiO_2$ could hardly adsorb methyl orange. All supported photocatalysts exhibited greater adsorption than bare $TiO_2$, indicating the importance of increased surface area in adsorption. The adsorption capacities of the corresponding 30%$TiO_2$/χHZSM-5 nano-composites increased constantly from 2.92 to 5.71% with increasing HCl concentration ranging from 0.1 to 1 mol/l during treatment.

### 3.2. Photocatalytic degradation

Total methyl orange removal is composed of two parts, adsorption on photocatalyst and photocatalytic degradation. The adsorption of MO on the photocatalyst is shown in Table 2. In the following statements, MO removal is solely the contribution of photocatalytic degradation. Fig. 4 shows the influence of HCl concentration on methyl orange degradation rate by varying HCl concentration from 0.1 to 2 mol/l. The degradation rate of MO

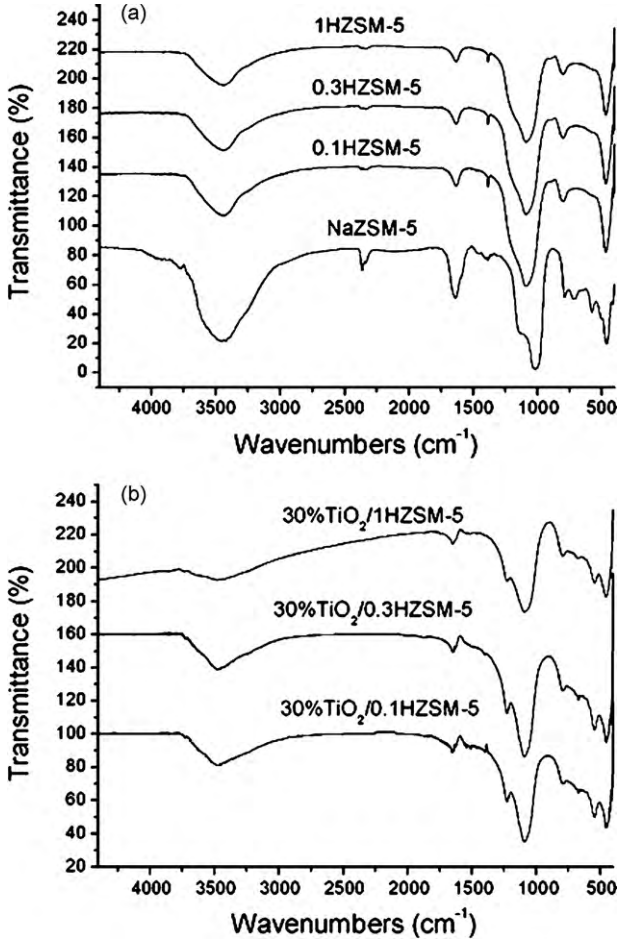


**Fig. 3.** FT-IR spectra of (a) ZSM-5 and (b) 30%$TiO_2$/$\chi$HZSM-5.

solution increased significantly from 22.2 to 36.5% when HCl concentration increased at a range from 0 to 0.3 mol/l, and then decreased with further increase of HCl concentration, although the adsorption of MO increased. MO molecules can be adsorbed directly on catalyst surface. However, too strong adsorption is unfavorable possibly for two reasons: poor migration of the adsorbed dye molecules on the surface, and ineffective activation of $TiO_2$ due to the blockage of UV light by large dye molecules [32]. Therefore, 0.3 mol/l can be the optimum HCl concentration in the treatment of NaZSM-5 zeolite as a support for $TiO_2$.

The effect of photocatalyst concentration on methyl orange degradation rate was studied by varying $TiO_2$ concentration from 0.1 to 1.6 g/l, as illustrated in Fig. 5. The degradation rate increased significantly from 11.2 to 42.5% with increasing $TiO_2$ concentration

**Table 2**
$TiO_2$ crystal size, BET surface area and adsorption of methyl orange.

| Sample | $TiO_2$ crystal size (nm)[a] | $S_{BET}$ ($m^2$/g) | Adsorption of methyl orange (%) |
|---|---|---|---|
| $TiO_2$ | 45.2 | 84.2 | 0.81 |
| NaZSM-5 | | 229.3 | 2.35 |
| 0.1HZSM-5 | | 298.7 | 3.26 |
| 0.3HZSM-5 | | 337.4 | 4.82 |
| 1HZSM-5 | | 346.7 | 6.34 |
| 30%$TiO_2$/NaZSM-5 | 18.3 | 115.7 | 1.72 |
| 30%$TiO_2$/0.1HZSM-5 | 19.4 | 179.7 | 2.92 |
| 30%$TiO_2$/0.3HZSM-5 | 19.7 | 239.6 | 4.11 |
| 30%$TiO_2$/1HZSM-5 | 18.4 | 242.9 | 5.71 |

[a] Calculated from (1 0 1) diffraction peak of anatase $TiO_2$ using Scherrer's equation.

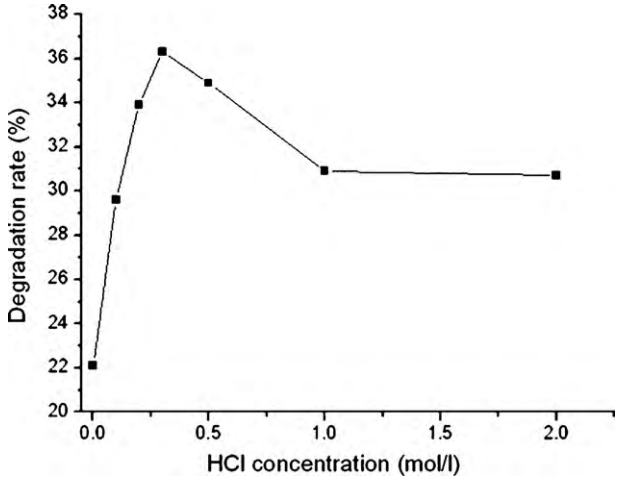


**Fig. 4.** Photocatalytic degradation of methyl orange as a factor of HCl concentration ($TiO_2$ concentration was 0.5 g/l for all photocatalysts).

at a range from 0.1 to 1.0 g/l and increased quite slowly afterwards due to light scattering and screening effect of suspended photocatalyst particles. It is suggested that at low level of photocatalyst concentration, increasing amount of photocatalyst can provide more reactive sites that are responsible for the enhancement of degradation efficiency. However, the solution becomes cloudy and opaque at high level of photocatalyst concentration, leading to reduced light penetration and available active site [33]. The increase of concentration may also result in the agglomeration of photocatalyst particles so that part of the photocatalyst surface becomes unavailable for photon absorption and dye adsorption.

Fig. 6 shows the relationship between methyl orange degradation and irradiation time for pure $TiO_2$ and 30%$TiO_2$/0.3HZSM-5 at 0.5 g/l of $TiO_2$ dosage. Photocatalytic activity of HZSM-5 was also studied as comparison. When using 2 g/l of HZSM-5, methyl orange degradation rate was less than 1% after 150 min of irradiation. HZSM-5 zeolite has very weak photocatalytic activity on methyl orange degradation under UV irradiation. Methyl orange degradation rates increased with irradiation time using either pure $TiO_2$ or 30%$TiO_2$/0.3HZSM-5. After 150 min of irradiation, methyl orange degradation rate was 99.5% using 30%$TiO_2$/0.3HZSM-5 composite as photocatalyst. Methyl orange degradation rate of pure $TiO_2$ under the same condition was much lower than 30%$TiO_2$/0.3HZSM-5 composite. The results show that photocatalytic activity of $TiO_2$ is improved by supporting it on HZSM-5 zeolite.

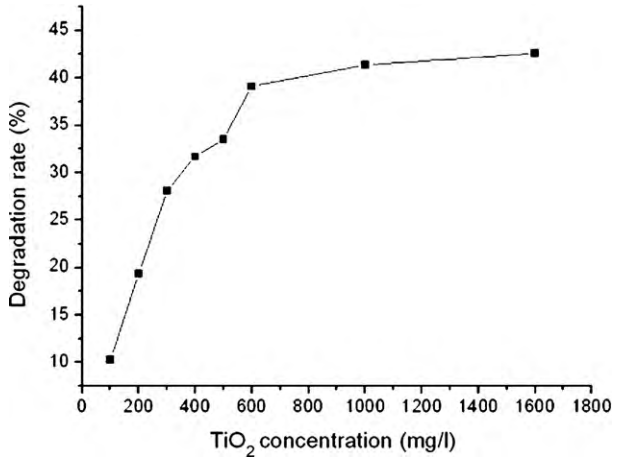


**Fig. 5.** $TiO_2$ concentration on methyl orange photocatalytic degradation using 30%$TiO_2$/0.3HZSM-5.

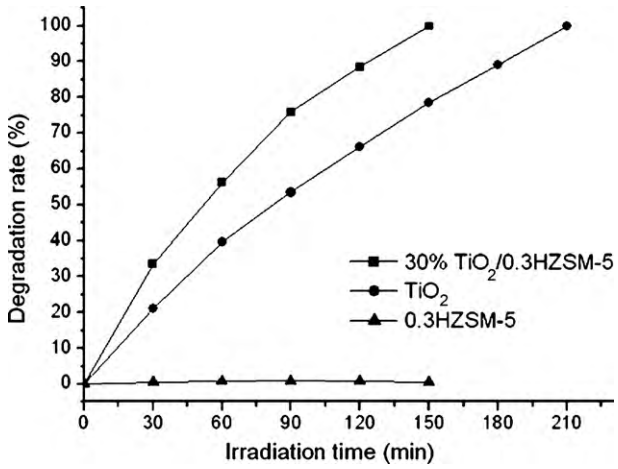


**Fig. 6.** Methyl orange photocatalytic degradation with prolonged irradiation time.

UV–visible spectra of methyl orange solution after irradiation on $TiO_2$ and 30%$TiO_2$/0.3HZSM-5 are shown in Fig. 7. The absorption peaks in UV and visible regions shrank as the irradiation time increased, indicating the disappearance of the corresponding functional groups of methyl orange molecules.

The recycling of photocatalyst is a very important parameter to assess the photocatalyst practicability. In our experiment, recycling of 30%$TiO_2$/0.3HZSM-5 was performed, as shown in Fig. 8. The photocatalyst was recycled after filtration and heating treatment at

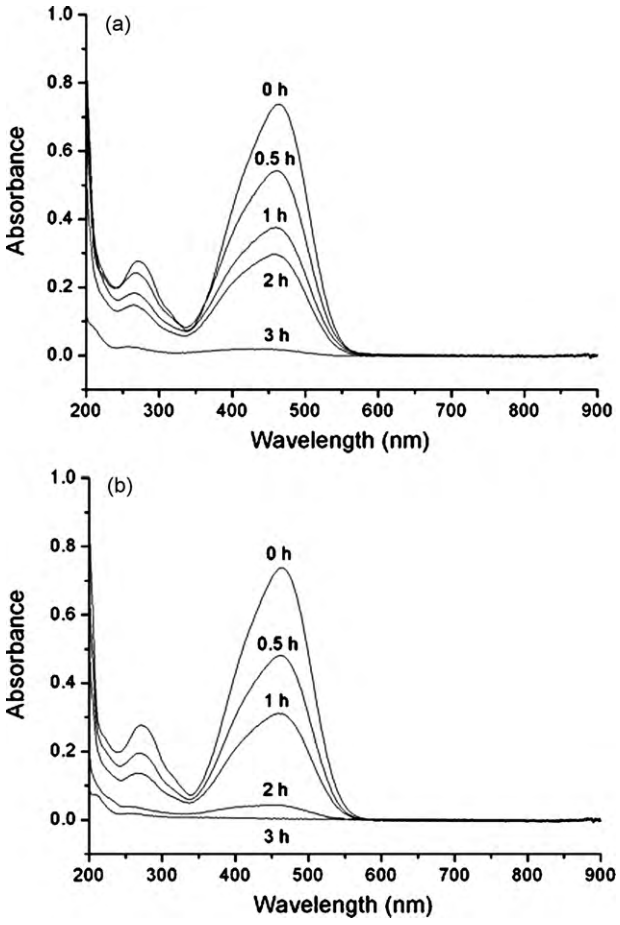


**Fig. 7.** UV–visible spectra of methyl orange solution after irradiation on (a) $TiO_2$ and (b) 30%$TiO_2$/0.3HZSM-5.

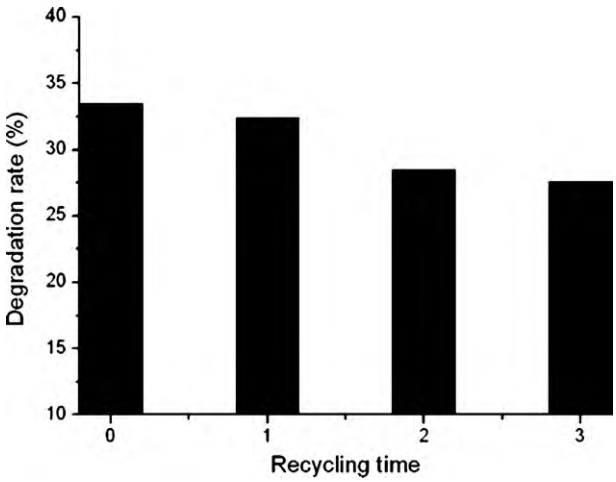


**Fig. 8.** Recycling of 30%$TiO_2$/0.3HZSM-5 on methyl orange photocatalytic degradation.

200 °C for 2 h in every cycle. After four cycles, methyl orange degradation rate decreased from 33.5 to 27.6%, maintaining 82.4% of the initial activity. The decrease of photocatalytic activity was due to $TiO_2$ loss from the zeolite surface and the fouling of the photocatalyst by by-products during degradation [33]. The $TiO_2$ attached on the zeolite may lose during filtrating and washing processes. Heat treatment can cause the elimination of by-products, and refresh the photocatalyst surface, resulting in recovery of photocatalytic activity. On the other hand, heat treatment can also induce photocatalyst aggregation after several recycles and lead to decrease of surface area and photocatalytic efficiency.

## 4. Conclusions

$TiO_2$ was dispersed using sol–gel method on the surfaces of a series of HZSM-5 zeolite supports treated by different concentrations of HCl. The modification of supports by HCl did not affect the zeolite's structure. The surface areas of the zeolite and the $TiO_2$/HZSM-5 nano-composite increased with increasing HCl concentration during treatment. The adsorption ability and photocatalytic activity of $TiO_2$/HZSM-5 were better than that of bare $TiO_2$. The optimum concentration of HCl in treating NaZSM-5 zeolite was 0.3 mol/l. The composite photocatalyst had good photocatalytic activity after three recycles.

## Acknowledgment

This work was supported by the National Natural Science Foundation of China (No. 50774074).

## Appendix A. Supplementary data

Supplementary data associated with this article can be found, in the online version, at doi:10.1016/j.cej.2010.07.042.

## References

[1] D. Chatterjee, S. Dasgupta, Visible light induced photocatalytic degradation of organic pollutants, J. Photochem. Photobiol. C 6 (2005) 186–205.
[2] V. Ramaswamy, N.B. Jagtap, S. Vijayanand, D.S. Bhange, P.S. Awati, Photocatalytic decomposition of methylene blue on nanocrystalline titania prepared by different methods, Mater. Res. Bull. 43 (2008) 1145–1152.
[3] A. Fujishima, T.N. Rao, D.A. Tryk, Titanium dioxide photocatalysis, J. Photochem. Photobio. C 1 (2000) 1–21.
[4] R.M. Mohamed, A.A. Ismail, I. Othmanb, I.A. Ibrahim, Preparation of $TiO_2$–ZSM-5 zeolite for photodegradation of EDTA, J. Mol. Catal. A 238 (2005) 151–157.

[5] W.J. Zhang, Y. Li, F.H. Wang, Properties of $TiO_2$ thin films prepared by magnetron sputtering, J. Mater. Sci. Technol. 18 (2002) 101–107.
[6] R. Portela, M.C. Canela, B. Sanchez, F.C. Marques, A.M. Stumbo, R.F. Tessinari, J.M. Coronado, S. Suarez, $H_2S$ photodegradation by $TiO_2$/M-MCM-41 (M=Cr or Ce): Deactivation and by-product generation under UV-A and visible light, Appl. Catal. B 84 (2008) 643–650.
[7] J. Schwitzgebel, J.G. Ekerdt, H. Gerischer, A. Heller, Role of the oxygen molecule and of the photogenerated electron in $TiO_2$-photocatalyzed air oxidation reactions, J. Phys. Chem. 99 (1995) 5633–5638.
[8] J. Saiena, M. Asgari, A.R. Soleymania, N. Taghavinia, Photocatalytic decomposition of direct red 16 and kinetics analysis in a conic body packed bed reactor with nanostructure titania coated Raschig rings, Chem. Eng. J. 151 (2009) 295–301.
[9] Saepurahman, M.A. Abdullah, F.K. Chong, Dual-effects of adsorption and photodegradation of methylene blue by tungsten-loaded titanium dioxide, Chem. Eng. J. 158 (2010) 418–425.
[10] M. Hussain, R. Ceccarelli, D.L. Marchisio, D. Fino, N. Russo, F. Geobaldo, Synthesis, characterization, and photocatalytic application of novel $TiO_2$ nanoparticles, Chem. Eng. J. 157 (2010) 45–51.
[11] T.A. McMurray, P. Dunlop, J.A. Byrne, The photocatalytic degradation of atrazine on nanoparticulate $TiO_2$ films, J. Photochem. Photobiol. A 182 (2006) 43–51.
[12] Z.S. Guan, X.T. Zhang, Y. Ma, Y.A. Cao, J.N. Yao, Photocatalytic activity of $TiO_2$ prepared at low temperature by a photoassisted sol–gel method, J. Mater. Res. 16 (2001) 907–909.
[13] H. Yahiro, T. Miyamoto, N. Watanabe, H. Yamaura, Photocatalytic partial oxidation of α-methylstyrene over $TiO_2$ supported on zeolites, Catal. Today 120 (2007) 158–162.
[14] M. Mahalakshmi, S.V. Priya, B. Arabindoo, M. Palanichamy, V. Murugesan, Photocatalytic degradation of aqueous propoxur solution using $TiO_2$ and H zeolite-supported $TiO_2$, J. Hazard. Mater. 161 (2009) 336–343.
[15] K. Yamaguchi, K. Inumaru, Y. Oumi, T. Sano, S. Yamanaka, Photocatalytic decomposition of 2-propanol in air by mechanical mixtures of $TiO_2$ crystalline particles and silicalite adsorbent: the complete conversion of organic molecules strongly adsorbed within zeolitic channels, Micropor. Mesopor. Mater. 117 (2009) 350–355.
[16] K. Tanaka, J. Fukuyoshi, H. Segawa, K. Yoshida, Improved photocatalytic activity of zeolite- and silica-incorporated $TiO_2$ film, J. Hazard. Mater. 137 (2006) 947–951.
[17] H. Chen, A. Matsumoto, N. Nishimiya, K. Tsutsumi, Preparation and characterization of $TiO_2$ incorporated Y-zeolite, Colloids Surf. 157 (1999) 295–305.
[18] X. Liu, K. Kong Iu, J.K. Thomas, Encapsulation of $TiO_2$ in zeolite Y, Chem. Phys. Lett. 195 (1992) 163–168.
[19] X. Liu, K. Kong Iu, J.K. Thomas, Preparation, characterization and photoreactivity of titanium(IV) oxide encapsulated in zeolites, J. Chem. Soc. Faraday Trans. 89 (1993) 1861–1865.
[20] V. Durga Kumari, M. Subrahmanyam, K.V. Subba Rao, A. Ratnamala, M. Noorjahan, K. Tanaka, An easy and efficient use of $TiO_2$ supported HZSM-5 and $TiO_2$ + HZSM-5 zeolite combinate in the photodegradation of aqueous phenol and p-chlorophenol, Appl. Catal. A 234 (2002) 155–165.
[21] M.V. Phanikrishna Sharma, K. Lalitha, V. Durga Kumari, M. Subrahmanyam, Solar photocatalytic mineralization of isoproturon over $TiO_2$/HY composite systems, Sol. Energy Mater. Sol. Cells 92 (2008) 332–342.
[22] M.V. Phanikrishna Sharma, V. Durga Kumari, M. Subrahmanyam, Solar photocatalytic degradation of isoproturon over $TiO_2$/H-MOR composite systems, J. Hazard. Mater. 160 (2008) 568–575.
[23] M.V. Phanikrishna Sharma, V. Durga Kumari, M. Subrahmanyam, Photocatalytic degradation of isoproturon herbicide over $TiO_2$/Al-MCM-41 composite systems using solar light, Chemosphere 72 (2008) 644–651.
[24] M. Nikazar, K. Gholivand, K. Mahanpoor, Photocatalytic degradation of azo dye Acid Red 114 in water with $TiO_2$ supported on clinoptilolite as a catalyst, Desalination 219 (2008) 293–300.
[25] A.C. Akah, G. Nkeng, A.A. Garforth, The role of Al and strong acidity in the selective catalytic oxidation of $NH_3$ over Fe-ZSM-5, Appl. Catal. B 74 (2007) 34–39.
[26] J.Y. Wang, F.Y. Zhao, R.J. Liu, Yong-Qi Hu, Oxidation of cyclohexane catalyzed by metal-containing ZSM-5 in ionic liquid, J. Mol. Catal. A 279 (2008) 153–158.
[27] P.O. Graf, L. Lefferts, Reactive separation of ethylene from the effluent gas of methane oxidative coupling via alkylation of benzene to ethylbenzene on ZSM-5, Chem. Eng. Sci. 64 (2009) 2773–2780.
[28] J. Pouilleau, D. Devilliers, H. Groult, P. Marcus, Surface study of a titanium-based ceramic electrode material by X-ray photoelectron spectroscopy, J. Mater. Sci. 32 (1997) 5645–5651.
[29] B.M. Reddy, I. Ganesh, E.P. Reddy, Study of dispersion and thermal stability of $V_2O_5/TiO_2$–$SiO_2$ catalysts by XPS and other techniques, J. Phys. Chem. B 101 (1997) 1769–1774.
[30] B.M. Reddy, B. Chowdhury, E.P. Reddy, A. Fernández, Vanadia–chromia grafted on titania: structural and catalytic properties in the selective catalytic reduction of NO by $NH_3$, J. Mol. Catal. A 162 (2000) 423–430.
[31] C.M. Zhu, L.Y. Wang, L.R. Kong, X. Yang, L.S. Wang, S. Zheng, F.L. Chen, F.M. Zhi, H. Zong, Photocatalytic degradation of azo dyes by supported $TiO_2$ + UV in aqueous solution, Chemosphere 41 (2000) 303–309.
[32] G. Li, X.S. Zhao, M.B. Ray, Advanced oxidation of orange II using $TiO_2$ supported on porous adsorbents: The role of pH, $H_2O_2$ and $O_3$, Sep. Purif. Technol. 55 (2007) 91–97.
[33] M.L. Huang, C.F. Xu, Z.B. Wu, Y.F. Huang, J.M. Lin, J.H. Wu, Photocatalytic discolorization of methyl orange solution by Pt modified $TiO_2$ loaded on natural zeolite, Dyes Pigments 77 (2008) 327–334.